

FOR THE RECORD

The dimeric form of the unphosphorylated response regulator BaeR

Hassanul G. Choudhury^{1,2,3} and Konstantinos Beis^{1,2,3*}

¹Division of Molecular Biosciences, Imperial College London, London, South Kensington, SW7 2AZ, United Kingdom

²Membrane Protein Lab, Diamond Light Source, Harwell Science and Innovation Campus, Chilton, Oxfordshire, OX11 0DE, United Kingdom

³Research Complex at Harwell, Harwell Oxford, Didcot, Oxfordshire OX11 0FA, United Kingdom

Received 13 May 2013; Accepted 8 July 2013
DOI: 10.1002/pro.2311
Published online 19 July 2013 proteinscience.org

Abstract: Bacterial response regulators (RRs) can regulate the expression of genes that confer antibiotic resistance; they contain a receiver and an effector domain and their ability to bind DNA is based on the dimerization state. This is triggered by phosphorylation of the receiver domain by a kinase. However, even in the absence of phosphorylation RRs can exist in equilibrium between monomers and dimers with phosphorylation shifting the equilibrium toward the dimer form. We have determined the crystal structure of the unphosphorylated dimeric BaeR from *Escherichia coli*. The dimer interface is formed by a domain swap at the receiver domain. In comparison with the unphosphorylated dimeric PhoP from *Mycobacterium tuberculosis*, BaeR displays an asymmetry of the effector domains.

Keywords: unphosphorylated response regulator; domain swap receiver domain; asymmetric dimer; effector domain

Introduction

Multidrug resistance is a growing problem in the treatment of infectious diseases and pathogenic bacteria have developed several mechanisms to confer resistance to antibiotics. Bacteria respond to antibiotics by regulating the expression of genes that code for various membrane bound multidrug resistant pumps and transporters. These pumps

and transporters are able to extrude structurally unrelated antibiotics and drugs and their expression is regulated on the transcription level.^{1–6} One of the mechanisms that bacteria utilize for regulating the gene expression is the two-component signal transduction system (TCS).⁷ The TCS comprises of a histidine kinase (HK) and a response regulator (RR).

BaeSR belongs to the TCS that activates transcription of the *mdtABC* and the *acrD* multidrug efflux pump genes^{8,9} and increases resistance to deoxycholate, indole, and novobiocin in *Escherichia coli*^{10,11} and in addition to oxacillin, cloxacillin, and nafcillin in an Δ *acrAB* strain of *Salmonella enterica*.¹² The BaeSR system can also sense copper and zinc suggesting a possible role for detoxification in *S. enterica* through the MdtABC and the AcrD pumps.¹³

Abbreviations: HK, histidine kinase; RR, response regulator; TCS, two-component signal transduction system.

Additional Supporting Information may be found in the online version of this article.

*Correspondence to: Konstantinos Beis, Membrane Protein Lab, Diamond Light Source, Harwell Science and Innovation Campus, Chilton, Oxfordshire, OX11 0DE, UK. E-mail: kbeis@imperial.ac.uk

The *S. enterica* BaeSR and CpxAR influence the outer membrane protein OmpD and confer resistance to ceftriaxone.¹⁴ The *spy* gene which encodes for a periplasmic chaperone is also under the same influence.¹⁵

BaeR belongs to the OmpR/PhoB family of transcription factor RRs.¹⁶ The RR consists of a receiver and an effector domain that are linked together through a flexible linker. The N-terminal receiver domain contains the conserved aspartate and the C-terminal effector domain is a DNA-binding domain involved in the transcriptional regulation of genes. There are many structures of isolated receiver and effector domains from the OmpR/PhoB family but only a few full length ones.^{17–22} Based on the phosphorylation state of the key Asp and orientation of the switch residues, Tyr/Phe and Ser/Thr, in the receiver domain, they can be classified as active or inactive²³ and this is linked with dimerization which is essential for binding DNA. RRs exist in equilibrium between active and inactive states and the equilibrium is shifted toward the active state upon phosphorylation. Phosphorylation of the RR triggers dimerization at their $\alpha 4$ - $\beta 5$ - $\alpha 5$ face of the receiver domain^{24,25} and it has been shown to be essential for regulation. In monomeric inactive RR structures, OmpR/PhoB family, the receiver and effector domains show interdomain contacts involving the switch residues with the exception of DrrD.¹⁷ The interdomain contacts in the inactive RRs have been proposed to represent an inhibitory state since the effector domains cannot dimerize without steric clashes. Activation would require disruption of this interface and it has been proposed that phosphorylation of the receiver domain and rotation of the switch residues would relieve the interdomain contacts, allowing formation of the dimer interface and subsequently transmitting changes to the effector domain.²⁰ In the inactive dimeric structure of PhoP from *Mycobacterium tuberculosis* there are no interdomain contacts and the dimer is formed by the $\alpha 4$ - $\beta 5$ - $\alpha 5$ face.²² To-date there is no structure of a full length active RR from the OmpR/PhoB family.

In this study, we determined the crystal structure of the full length BaeR from *E. coli* at 3.3 Å resolution. The crystal structure shows a very compact domain swap dimer in the receiver domain. The unphosphorylated BaeR structure is a dimer and does not display any interdomain contacts.

Results

Overall structure of BaeR

The structure of full length BaeR from *E. coli* was determined using experimental phases from single wavelength anomalous dispersion dataset ($\lambda = 1.255$ Å) from a holmium derivatized protein co-crystal soaked in 20 mM Ta₆Br₁₂ cluster at 3.3 Å resolution in the C2 space group (Supporting Information Fig.

S1A). The asymmetric unit contains 12 copies of BaeR related by a sixfold non-crystallographic symmetry (NCS) axis. We found that it was necessary to co-crystallize the protein with holmium in order to improve the diffraction quality of the crystals. The diffraction quality improved further after soaking them in the tantalum cluster. Data at low resolution, 3.8–4.0 Å resolution, were also collected for the native, selenomethionine, and holmium derivatized proteins. The holmium derivatized protein and tantalum cluster soaks resulted in breaking the symmetry from *P3₁21* to *C2* symmetry which improved the diffraction by slight rearrangements in the crystal packing; comparison of the BaeR molecules between the two different space groups did not reveal any structural differences. During the refinement and model building, we noticed extra electron density for all the cysteines, and we assigned it to arsenic (anomalous difference maps) from the cacodylate buffer (Supporting Information Fig. S1B).

In the crystal structure, BaeR is in dimeric form (Fig. 1) and the two protomers are related by a twofold rotational symmetry. The overall structure of BaeR resembles other full-length RR proteins of the OmpR/PhoB family; it contains an N-terminal receiver domain (residues 10–126) and a C-terminal effector DNA-binding domain (residues 141–240). The two domains are connected together by a linker of 15 residues in length; in our electron density maps we can observe some density for the linker but the resolution is not sufficient to be built (Supporting Information Fig. S2). Receiver domains of RRs comprise of a five-stranded β -core flanked by five α -helices and have a characteristic $\beta 1$ - $\alpha 1$ - $\beta 2$ - $\alpha 2$ - $\beta 3$ - $\alpha 3$ - $\beta 4$ - $\alpha 4$ - $\beta 5$ - $\alpha 5$ topology²² [Fig. 2(A)]. The receiver domain of BaeR is incomplete with topology $\beta 1$ - $\alpha 1$ - $\beta 2$ - $\alpha 2$ - $\beta 3$ - $\alpha 3$ - $\beta 4$ - $\alpha 5$. The complete receiver domain is formed from a domain swap with the second protomer that provides the $\alpha 4$ - $\beta 5$ elements. Domain swapping has been reported before for another RR, RegX3 that also forms a domain-swap dimer in its receiver domain²¹; the complete receiver domain is formed from the $\beta 1$ - $\alpha 1$ - $\beta 2$ - $\alpha 2$ - $\beta 3$ - $\alpha 3$ - $\beta 4$ of the first molecule and the $\alpha 4$ - $\beta 5$ - $\alpha 5$ elements are provided from the domain swap with the second molecule. In BaeR, the domain swapped region has a buried surface of 1370 Å²/protomer whereas RegX3 has 2357 Å²/protomer. $\beta 5$ of the incomplete receiver domain aligns parallel to the domain-swapped four β -sheet core and forms a complete five stranded core. In BaeR structure, helix $\alpha 4$ (residues 92–101) has completely unwound; for consistency with the other published structures and for discussion purposes, it will be referred as “helix $\alpha 4$.” The unwound “helix $\alpha 4$ ” sits adjacent to the $\alpha 3$ of the domain swap dimer. The two receiver domains of the BaeR dimer can be

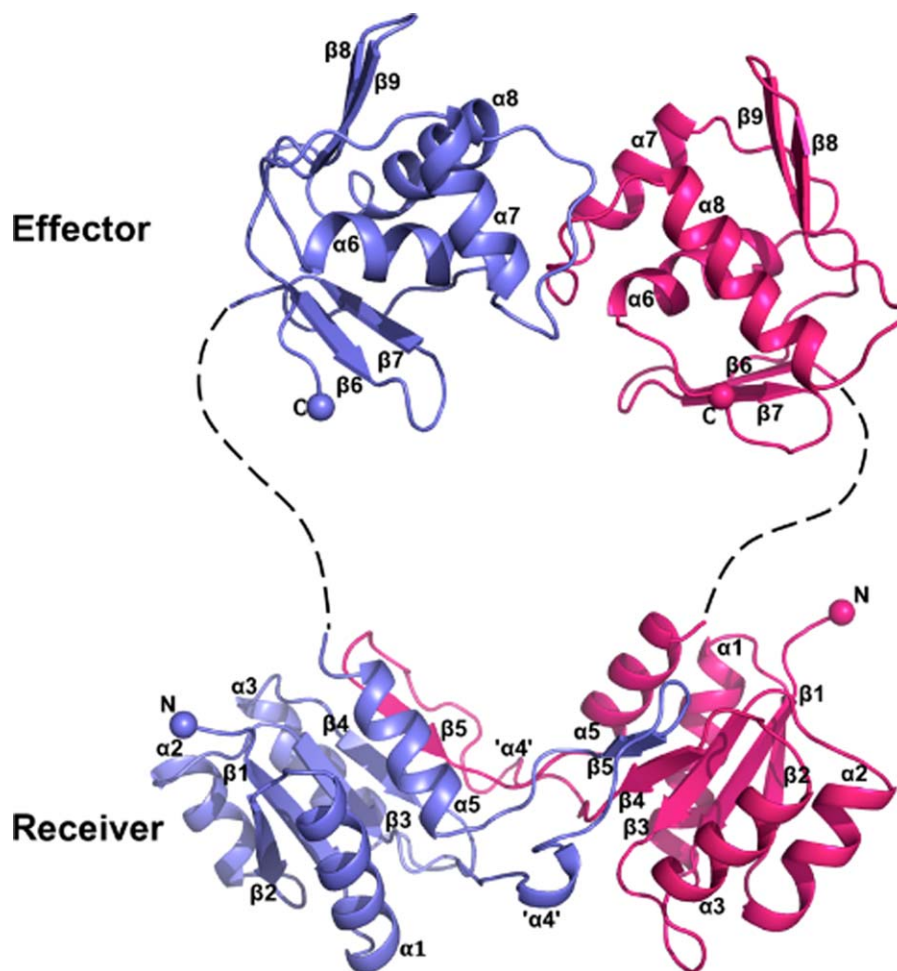


Figure 1. Ribbon representation of the BaeR dimer. One protomer is shown in light blue and the other in magenta. The linker region is missing from the final structure but for visualization purposes we have drawn it as dotted line (Supporting Information Fig. S2). The complete receiver domain is formed from a domain swap between the β -core domain and α 4- β 5. An interactive view is available in the electronic version of the article. [Color figure can be viewed in the online issue, which is available at wileyonlinelibrary.com.]

superimposed with an rmsd of 2.55 Å over 110 C_{α} atoms. Closer inspection of the phosphorylation site β 3- α 3 reveals that the two protomers show structural differences; residues 62–68 have been flipped over by 80° and then displaced by 8.0 Å relative to each other.

The overall structure of the BaeR effector domain is very similar to other effector domains of full length RRs of the OmpR/PhoB family.¹⁷ It has a winged helix-turn-helix (wHTH) motif consisting of a two-stranded antiparallel β -sheet followed by a three-helix bundle and a C-terminal β -hairpin (Fig. 1). Helix α 8 is the recognition helix that interacts with the DNA and its accessibility to bind DNA is determined by the conformation of the transactivation loop (involved in transcription activation) between α 7 and α 8; in BaeR, the current conformation prevents it from binding DNA. The effector domain is linked to the receiver domain through a long linker but the two domains do not have any interdomain contacts.

Unwound “helix α 4”

A striking feature of BaeR is that helix α 4 of the receiver domain is completely unwound in both protomers (Fig. 1). The structural plasticity of α 4 has been previously reported.²⁶ Helix α 4 is usually positioned parallel to the five-stranded β -sheet core of the receiver domain but in DrrD it has been displaced and adopted an almost perpendicular configuration relative to the five-stranded β -sheet core as a result of the rotation of the α 4 helical segment about its own axis¹⁷ [Fig. 2(B,C)]. In BaeR, the unwound “helix α 4” is sitting perpendicular to the β -sheet core domain; the hydrophobic residues are pointing toward the hydrophobic core of the adjacent domain swapped dimer compensating for the unwinding. In turn, β 5 is also forced to adopt the same perpendicular orientation and is displaced from the core domain. Interactions from α 3 of the domain swapped dimer place the unwound helix parallel to the hydrophobic core to form the complete receiver domain.

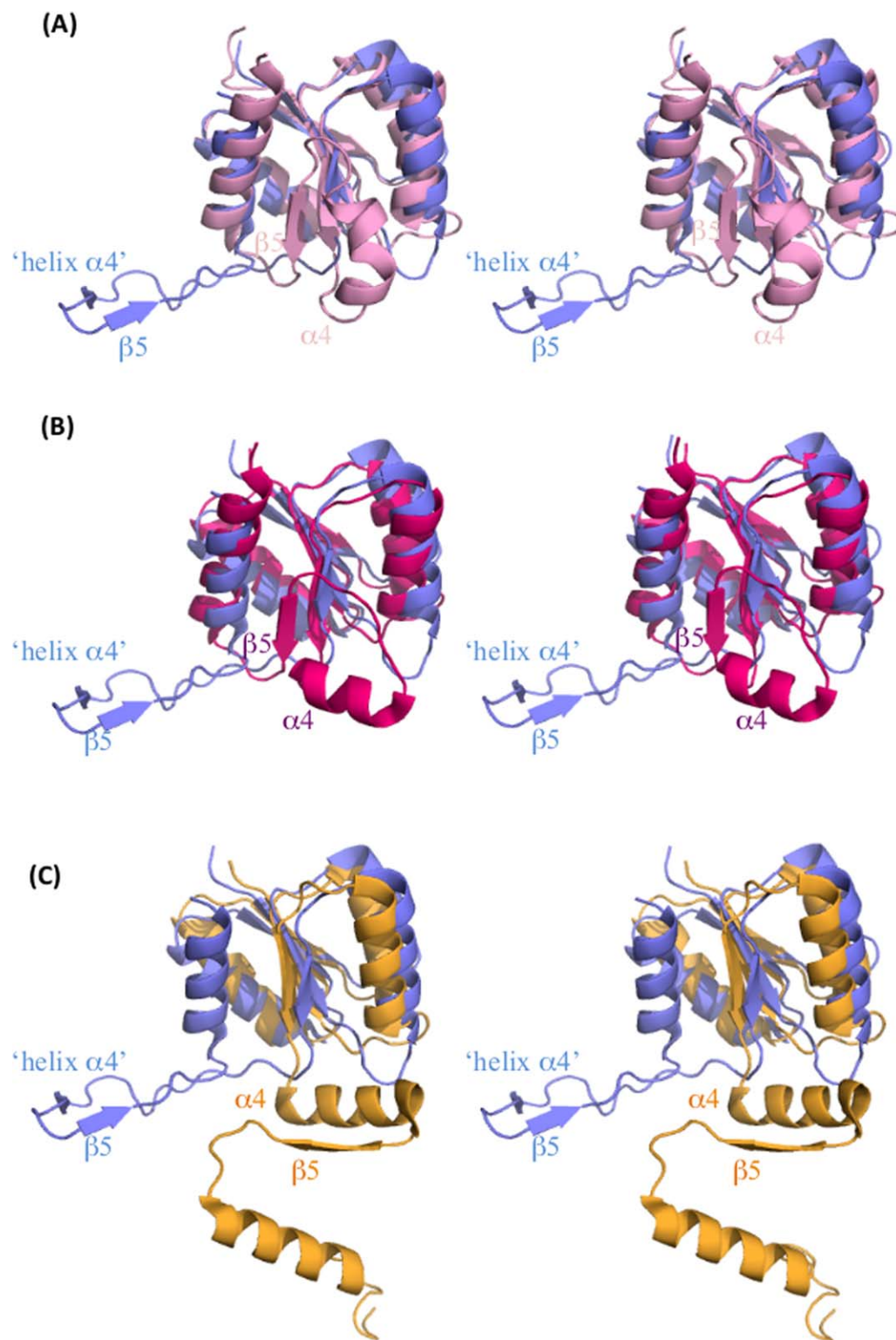


Figure 2. Structural differences in the receiver domain of RRs. Stereo-representation of the superimposed receiver domain of BaeR (blue) with (A) PhoP (pink, PDB ID 3R0J), (B) DrrD (magenta, PDB ID 1KGS), and (C) RegX3 (yellow, PDB ID 2OQR). Only the “helix $\alpha 4$ ”- $\beta 5$ and equivalent elements are labeled. $\alpha 4$ of DrrD is sitting perpendicular to the β -core domain. In BaeR, rotation along the N-terminus of $\alpha 5$ has allowed the “helix $\alpha 4$ ”- $\beta 5$ elements to swing out of the core domain. The $\alpha 4$ - $\beta 5$ - $\alpha 5$ elements of RegX3 are involved in the domain swap. [Color figure can be viewed in the online issue, which is available at wileyonlinelibrary.com.]

This hydrophobic pocket is formed from Ile94, Leu97, and Leu100 of the unwound $\alpha 4$ and Leu62 and Leu70 from the domain swapped $\alpha 3$. The side chain

of Arg96 and main chain of Asp105 form a hydrogen bond with the main chain of Leu62 and the side chain of the domain swapped Arg77, respectively.

Glu93 forms a hydrogen bond with Tyr29 from helix $\alpha 1$ of the same molecule. The interactions from the main molecule and the domain swapped protomer appear to stabilize the unwound helix (Supporting Information Fig. S3).

Discussion

BaeR represents the second example of a domain swapped dimer of a full length RR of the OmpR/PhoB family. The formation of RR domain swapped dimers in RegX3 has been previously associated with high protein concentrations or crystallization conditions.^{21,25} Both RegX3 and BaeR protein structures have a complete active site for phosphorylation which can be linked to the mechanism of activation via the switch residues (Supporting Information Fig. S4). The intrinsic plasticity of helix $\alpha 4$ has been previously reported and in our structure it is completely unwound. We cannot exclude that formation of the domain swapped dimer is due to the flexible nature of $\alpha 4$. Upon phosphorylation $\alpha 4$ could be stabilized and adopt a more helical conformation which would also bring $\beta 5$ to the core domain and disrupt the domain swap.

In order for RRs to bind their target DNA, they need to dimerize. Unphosphorylated RRs exist in equilibrium between monomers and dimers, and phosphorylation pushes the equilibrium toward dimer, which is associated with DNA binding. Dimerization of the RRs, OmpR/PhoB family, usually involves the $\alpha 4$ - $\beta 5$ - $\alpha 5$ face of the receiver domain. The BaeR dimer interface is formed between the $\alpha 4$ and $\beta 5$ face elements from the domain swapped dimers. Isolated beryllium fluoride activated receiver domains usually dimerize in a face-to-face orientation. The BaeR dimers sit almost 90° from one another as a result of the domain swap suggesting a novel way of dimerization but with the same elements as observed in other structures. The fully phosphorylated BaeR might result in a tighter dimer interface; the inactive PhoP dimerizes at the $\alpha 4$ - $\beta 5$ - $\alpha 5$ face whereas the isolated activated receiver domain has a more compact interface.²² Some inactive RRs display interdomain contacts and are believed to be inhibitory in forming dimers; rotation of the switch residues would relieve these contacts and allow dimerization upon phosphorylation and bind DNA. The current domain organization of the BaeR dimer does not allow for any interdomain contacts since it would create steric clashes. In addition, the BaeR dimer has an asymmetric conformation between the receiver and effector domain relative to the PhoP dimer. This domain organization probably explains the ability of unphosphorylated BaeR to bind its target DNA.¹⁰

In our structure, the two effector domains form weak bonds through their transactivation loop, stabilizing the extended receiver-effector interface (crystal contacts). From the crystal structure of the isolated effector domain of PhoB bound to DNA, the

current conformation would prevent the protein from accessing the major groove. The PhoB binds to tandem repeat DNA half-sites with translational symmetry in a head-to-tail orientation.²⁷ For BaeR to bind DNA it would require re-orientation of the effector domains; the rather flexible linker and absence of interdomain contacts would easily allow re-orientation of the domain in the presence of DNA. Another possible mode of binding would be in a face-to-face similar to the OmpR-DNA model.²⁸ The unwinding of the last turn of $\alpha 5$ permits the effector domains to freely rotate.

Materials and Methods

Cloning

Full length *baeR* from *E. coli* MG1655 was cloned into the pEHis/TEV vector. The sequenced clone had a Thr71Met mutation that we decided not to correct since we could use it in selenomethionine derivatization and phasing.

Overexpression and purification

BaeR was transformed in BL21(DE3) cells. Cells were grown in LB medium supplemented with 34 $\mu\text{g/L}$ kanamycin to an OD_{600} 0.8 at 300 K and expression was induced by adding 1 mM isopropyl-1-thio- β -D-galactopyranoside for further 4 h. Cells were harvested by centrifugation at 6,000g.

All purification steps were carried out at 277 K. Cells were broken using a Constant Cell Disruption system. The unbroken cells and cell membranes were removed by centrifugation at 150,000g for 1 h. The supernatant was adjusted to 20 mM imidazole and passed over a 5 mL His-trap column HP, equilibrated with three column volumes (CV) of 20 mM imidazole in phosphate buffered saline (PBS). The column was washed with five CV of 30 mM imidazole in PBS. The protein was eluted with five CV of 500 mM imidazole in PBS. The His₆-tag was cleaved from the protein using Tobacco Etch Virus (TEV) protease at a 1:100 ratio and dialyzed in 2 L of 20 mM Tris pH 7.5, 150 mM NaCl overnight with stirring. The dialyzed protein was passed over a 5 mL His-trap column equilibrated in dialysis buffer. The flow through was collected and injected over a Superdex 75 10/300 equilibrated in 20 mM Tris pH 8.0, 50 mM NaCl, and 5 mM dithiothreitol (DTT). The fractions containing BaeR were collected and concentrated using a 10 kDa concentrator.

Crystallization

Initial vapor diffusion sitting-drop crystallization trials were carried out using a Mosquito crystallization robot (TTP LabTech) from a protein solution at 30 mg/mL at 277 K and 293 K; 100 nL protein solution was mixed with 100 nL crystallization buffer. BaeR crystals appeared after 5 days in 1.2 M sodium

acetate and 0.1 M sodium cacodylate, pH 8.4 at 277 K. Crystal quality and size were improved by seeding pre-equilibrated hanging-drops (mixing 1 μ L protein with 1 μ L crystallization buffer) overnight at 277 K; the precipitant concentration was reduced by 5%. The diffraction quality of the crystals was further improved by co-crystallizing the protein with 1 mM Ho (III). Crystals were derivatized by adding 20 mM Ta₆Br₁₂ cluster (Jena Biosciences) to the crystallization drop and were soaked for 24 h.

Data collection and structure determination

Crystals were transferred into crystallization solution containing 20% glycerol and were flash frozen into liquid nitrogen prior to data collection. Data were collected at beamline ID14-4 at ERSF, I02 and I04 at Diamond Light Source. Data were processed with xia2.²⁹ The data collection statistics are summarized in Supporting Information Table S1.

Initial Ta heavy atom positions were determined by SHELXD³⁰ using a SAD dataset from a single crystal containing both Ta₆Br₁₂ and Ho at a wavelength of 1.255 Å; the sites were refined and initial phases were calculated using autoSHARP³¹ assuming solvent content of 70% and 12 copies of BaeR in the asymmetric unit. The selenomethionine data were used to calculate anomalous difference maps and the sites were used for correct tracing of the sequence (Supporting Information Table S2). At this stage data from a crystal containing only Ta₆Br₁₂ was obtained at 3.3 Å resolution and the current model was used as a search model for molecular replacement in Phaser.³² The model underwent multiple rounds of model building using Coot and refinement using Phenix refine.³³ In the last stages of refinement, the six dimers were restrained by sixfold NCS. The final model was refined to 3.3 Å resolution with an R_{factor} of 22.52% and R_{free} of 24.48%. The Ramachandran has 95.1% in favored regions, 4.66% in allowed, and 0.23% outliers as calculated by MolProbity. The Ramachandran outliers are in a loop region with poor density and correspond to a Gly.

The coordinates and structure factors have been deposited with the RCSB Protein Data Bank with PDB ID code 4B09.

Acknowledgments

Authors would like to acknowledge the Diamond Light Source and ESRF synchrotrons for beamtime. They would also like to thank Dr Alexander Cameron for critical reading of the manuscript.

References

1. Lomovskaya O, Lewis K, Matin A (1995) EmrR is a negative regulator of the *Escherichia coli* multidrug resistance pump EmrAB. *J Bacteriol* 177:2328–2334.

2. Ma D, Alberti M, Lynch C, Nikaido H, Hearst JE (1996) The local repressor AcrR plays a modulating role in the regulation of *acrAB* genes of *Escherichia coli* by global stress signals. *Mol Microbiol* 19:101–112.
3. Okusu H, Ma D, Nikaido H (1996) AcrAB efflux pump plays a major role in the antibiotic resistance phenotype of *Escherichia coli* multiple-antibiotic-resistance (Mar) mutants. *J Bacteriol* 178:306–308.
4. Tanaka T, Horii T, Shibayama K, Sato K, Ohsuka S, Arakawa Y, Yamaki K, Takagi K, Ohta M (1997) RobA-induced multiple antibiotic resistance largely depends on the activation of the AcrAB efflux. *Microbiol Immunol* 41:697–702.
5. White DG, Goldman JD, Demple B, Levy SB (1997) Role of the *acrAB* locus in organic solvent tolerance mediated by expression of *marA*, *soxS*, or *robA* in *Escherichia coli*. *J Bacteriol* 179:6122–6126.
6. Xiong A, Gottman A, Park C, Baetens M, Pandza S, Matin A (2000) The EmrR protein represses the *Escherichia coli* *emrRAB* multidrug resistance operon by directly binding to its promoter region. *Antimicrob Agents Chemother* 44:2905–2907.
7. Stock AM, Robinson VL, Goudreau PN (2000) Two-component signal transduction. *Annu Rev Biochem* 69:183–215.
8. Nagakubo S, Nishino K, Hirata T, Yamaguchi A (2002) The putative response regulator BaeR stimulates multidrug resistance of *Escherichia coli* via a novel multidrug exporter system, MdtABC. *J Bacteriol* 184:4161–4167.
9. Leblanc SK, Oates CW, Raivio TL (2011) Characterization of the induction and cellular role of the BaeSR two-component envelope stress response of *Escherichia coli*. *J Bacteriol* 193:3367–3375.
10. Baranova N, Nikaido H (2002) The baeSR two-component regulatory system activates transcription of the *yegMNOB* (*mdtABCD*) transporter gene cluster in *Escherichia coli* and increases its resistance to novobiocin and deoxycholate. *J Bacteriol* 184:4168–4176.
11. Hirakawa H, Inazumi Y, Masaki T, Hirata T, Yamaguchi A (2005) Indole induces the expression of multidrug exporter genes in *Escherichia coli*. *Mol Microbiol* 55:1113–1126.
12. Appia-Ayme C, Patrick EJ, Sullivan M, Alston MJ, Field SJ, Abuoun M, Anjum MF, Rowley G (2011) Novel inducers of the envelope stress response BaeSR in *Salmonella typhimurium*: BaeR is critically required for tungstate waste disposal. *PLoS One* 6:e23713.
13. Nishino K, Nikaido E, Yamaguchi A (2007) Regulation of multidrug efflux systems involved in multidrug and metal resistance of *Salmonella enterica* serovar Typhimurium. *J Bacteriol* 189:9066–9075.
14. Hu WS, Chen HW, Zhang RY, Huang CY, Shen CF (2011) The expression levels of outer membrane proteins STM1530 and OmpD, which are influenced by the CpxAR and BaeSR two-component systems, play important roles in the ceftriaxone resistance of *Salmonella enterica* serovar Typhimurium. *Antimicrob Agents Chemother* 55:3829–3837.
15. Yamamoto K, Ogasawara H, Ishihama A (2008) Involvement of multiple transcription factors for metal-induced *spy* gene expression in *Escherichia coli*. *J Biotechnol* 133:196–200.
16. Martinez-Hackert E, Stock AM (1997) Structural relationships in the OmpR family of winged-helix transcription factors. *J Mol Biol* 269:301–312.
17. Buckler DR, Zhou Y, Stock AM (2002) Evidence of intradomain and interdomain flexibility in an OmpR/

- PhoB homolog from *Thermotoga maritima*. *Structure* 10:153–164.
18. Robinson VL, Wu T, Stock AM (2003) Structural analysis of the domain interface in DrrB, a response regulator of the OmpR/PhoB subfamily. *J Bacteriol* 185:4186–4194.
 19. Nowak E, Panjikar S, Konarev P, Svergun DI, Tucker PA (2006) The structural basis of signal transduction for the response regulator PrrA from *Mycobacterium tuberculosis*. *J Biol Chem* 281:9659–9666.
 20. Friedland N, Mack TR, Yu M, Hung LW, Terwilliger TC, Waldo GS, Stock AM (2007) Domain orientation in the inactive response regulator *Mycobacterium tuberculosis* MtrA provides a barrier to activation. *Biochemistry* 46:6733–6743.
 21. King-Scott J, Nowak E, Mylonas E, Panjikar S, Roessle M, Svergun DI, Tucker PA (2007) The structure of a full-length response regulator from *Mycobacterium tuberculosis* in a stabilized three-dimensional domain-swapped, activated state. *J Biol Chem* 282:37717–37729.
 22. Menon S, Wang S (2011) Structure of the response regulator PhoP from *Mycobacterium tuberculosis* reveals a dimer through the receiver domain. *Biochemistry* 50:5948–5957.
 23. Bachhawat P, Swapna GV, Montelione GT, Stock AM (2005) Mechanism of activation for transcription factor PhoB suggested by different modes of dimerization in the inactive and active states. *Structure* 13:1353–1363.
 24. Toro-Roman A, Wu T, Stock AM (2005) A common dimerization interface in bacterial response regulators KdpE and TorR. *Protein Sci* 14:3077–3088.
 25. Gao R, Stock AM (2010) Molecular strategies for phosphorylation-mediated regulation of response regulator activity. *Curr Opin Microbiol* 13:160–167.
 26. Milani M, Leoni L, Rampioni G, Zennaro E, Ascenzi P, Bolognesi M (2005) An active-like structure in the unphosphorylated StyR response regulator suggests a phosphorylation-dependent allosteric activation mechanism. *Structure* 13:1289–1297.
 27. Blanco AG, Sola M, Gomis-Ruth FX, Coll M (2002) Tandem DNA recognition by PhoB, a two-component signal transduction transcriptional activator. *Structure* 10:701–713.
 28. Rhee JE, Sheng W, Morgan LK, Nolet R, Liao X, Kenney LJ (2008) Amino acids important for DNA recognition by the response regulator OmpR. *J Biol Chem* 283:8664–8677.
 29. Winter G (2010) xia2: an expert system for macromolecular crystallography data reduction. *J Appl Cryst* 43:186–190.
 30. Sheldrick GM (2008) A short history of SHELX. *Acta Cryst A* 64:112–122.
 31. Vonrhein C, Blanc E, Roversi P, Bricogne G (2007) Automated structure solution with autoSHARP. *Methods Mol Biol* 364:215–230.
 32. McCoy AJ, Grosse-Kunstleve RW, Adams PD, Winn MD, Storoni LC, Read RJ (2007) Phaser crystallographic software. *J Appl Cryst* 40:658–674.
 33. Adams PD, Afonine PV, Bunkoeci G, Chen VB, Davis IW, Echols N, Headd JJ, Hung LW, Kapral GJ, Grosse-Kunstleve RW, McCoy AJ, Moriarty NW, Oeffner R, Read RJ, Richardson DC, Richardson JS, Terwilliger TC, Zwart PH (2010) PHENIX: a comprehensive Python-based system for macromolecular structure solution. *Acta Cryst D* 66:213–221.